DOI 10.1007/s11141-017-9766-2
Radiophysics and Quantum Electronics, Vol. 59, No. 12, May, 2017
(Russian Original Vol. 59, No. 12, November, 2016)

ON FEATURES OF THE GENERATION OF ARTIFICIAL IONOSPHERIC IRREGULARITIES WITH TRANSVERSE SCALES OF 50–200 m

I. A. Bolotin,[1] **V. L. Frolov,** [1,2*] **A. D. Akchurin,**[2] **and E. Yu. Zykov** [2]

UDC 533.951+537.868

We consider the features of generation of artificial ionospheric irregularities with transverse (to the geomagnetic field) scales $l_\perp \approx 50$–200 m in the ionosphere modified by high-power HF radio waves. It was found that there are at least two mechanisms for generation of these irregularities in the ionospheric F region. The first mechanism is related to the resonant interaction between radio waves and the ionospheric plasma, while the second one takes place even in the absence of the resonant interaction. Different polarization of the high-power radiation was used to separate the mechanisms in the measurements.

1. INTRODUCTION

Among a variety of the effects observed during modification of the Earth's ionosphere by high-power radio waves, the generation of artificial ionospheric irregularities is one of the most important ones. They are excited in a wide range of transverse (to the geomagnetic field) scales (from fractions of a meter to ten or more kilometers) and affect the propagation of radio waves of different frequency ranges. The properties of these irregularities have been studied by many authors. These studies were the basis for determining the spectral characteristics during excitation of irregularities in the evening and nighttime conditions near the height of reflection of the O-mode high-power radio wave, when the pump-wave frequency is outside the regions of resonances with the electron gyrofrequency harmonics [1–4]. In particular, the existence of two spectral maxima was found, one of which is detected in the scale range $l_\perp \approx 30$–50 m and is due to the development of the thermal (resonant) parametric instability [5–7] and the second belongs to the scale range $l_\perp \approx 300$–800 m and is due to the self-focusing instability of the high-power radio wave [8–10]. The mechanism of generation of artificial ionospheric irregularities in the intermediate-scale range $l_\perp \approx 50$–200 m remained unexplored until recent time. It was shown in [11–13] that these irregularities have a high intensity and cause strong scattering of the probing radio waves of both polarizations which sound the disturbed ionospheric region at frequencies close to the pump-wave frequency.

This paper aims at determining the features of generation of artificial ionospheric irregularities with the scales $l_\perp \approx 50$–200 m. The experimental data considered in this paper were obtained for the ionosphere modified by means of the SURA heating facility. In Sec. 2, we present the methods of diagnostics of such irregularities and consider the capabilities and limitations of these techniques. Also, we discuss the ionospheric modification regimes which we used to solve the problem.

* frolov@nirfi.unn.ru

[1] Radiophysical Research Institute of the N. I. Lobachevsky State University of Nizhny Novgorod, Nizhny Novgorod; [2] Kazan (Volga) Federal University, Kazan, Russia. Translated from Izvestiya Vysshikh Uchebnykh Zavedenii, Radiofizika, Vol. 59, No. 12, pp. 1087–1097, November 2016. Original article submitted July 27, 2015; accepted March 8, 2016.

2. ORGANIZATION OF THE EXPERIMENTS

The main tool for diagnostics of artificial ionospheric irregularities with the scales $l_\perp \approx 50$–200 m in the SURA heater experiments is the modified ionosonde of the Physical Faculty of the Kazan (Volga) Federal University. Due to the wide radiation pattern, the ionosonde in the backscattering regime can probe the ionospheric region above the facility. The ionosonde signals scattered by the irregularities excited during the SURA operation manifest themselves in the ionograms in the form of additional diffusive traces, the analysis of which suggests some conclusions on the properties of the irregularities.

Favorable geographical position of the ionosonde plays an important role here. The point is that in the frequency range 1.4–7.0 MHz being used, due to the strong refraction of radio waves in the ionosphere, the measurements are best done when the receiver–transmitter complex is close enough to the heater (within half a hop for the probing radio waves). This ionosonde is specific in that in the pauses between taking ionograms it can be placed in the regime of probing at several fixed frequencies. This permits one to monitor the dynamics of the scattered signal and evaluate the development and relaxation times of the corresponding irregularities.

A more detailed description of the ionosonde and the features of the studies based on it are presented in [13]. It is also shown there that this method gives a unique opportunity for recording and diagnostics of artificial ionospheric irregularities in the scale range $l_\perp \approx 50$–200 m throughout the entire ionospheric depth (from the altitudes of the E region to the altitudes of the F_2-layer maximum). In the daytime hours, the scattering is observed, as a rule, only at frequencies above 4 MHz and has a low intensity. In the evening, and especially in the late evening hours of observation, the scattering intensity strongly increases, and the scattering occupies an increasingly broad frequency band, lowering to about 1.4 MHz.

It is clear that for such a geometry of the radar location and the disturbed ionospheric region, scattering by different-scale irregularities in the sounding frequency range being used occurs from different altitudes. For example, in the nighttime conditions, depending on the profile of the ionospheric-plasma density, scattering by irregularities with the scales $l_\perp \approx 50$–100 m occurs from altitudes above 200 km, scattering by irregularities with the scales $l_\perp \approx 100$–150 m, from altitudes 150–200 km, and scattering by irregularities with the scales $l_\perp \approx 200$ m, from altitudes below 150 km. In the daytime conditions, radio waves at frequencies below 4 MHz can sound only altitudes from 100 to 150 km, where they are scattered by irregularities with $l_\perp \approx 100$–200 m. The F_2 region can be sounded only at frequencies above 5 MHz, which corresponds to scattering by irregularities with the scale $l_\perp \approx 50$ m.

Some limitations of this method are mentioned in [13]. For example, scattered signals from the ionospheric F_2 region (especially at frequencies below 4–5 MHz) can only be recorded in the absence of high-power sporadic E layers, the appearance of which leads to screening of the disturbed regions at altitudes $h > 100$–130 km. For intense (opaque) sporadic E layers, sounding of the disturbed regions becomes possible.

When setting up experiments to study the features of generation of artificial ionospheric irregularities, we took into account the following properties of the artificial ionospheric turbulence excited during modification of the magnetized plasma by high-power radio waves. It is well known that when the upper ionosphere is affected by high-power HF O-mode radio waves at frequencies close to the electron gyrofrequency harmonic, double resonance takes place under certain conditions in the region of the high-power-wave — plasma interaction. In this case, the equality $\omega \approx n\omega_{ce} \approx \omega_{UH}(z)$ is fulfilled (here, ω is the pump-wave frequency, ω_{ce} is the electron gyrofrequency in the region of the high-power-wave — plasma interaction, n is an integer, and $\omega_{UH}(z)$ is the upper-hybrid frequency). Parametric interaction between a high-power radio wave and the plasma is suppressed in the upper-hybrid resonance region, and, as a consequence, the generation of small-scale ($l_\perp \approx 50$ m) irregularities is suppressed [14] and thermal components of the ionospheric stimulated radio emission (SEE) are excited [15–17]. The latter circumstance is used during measurements for seeking the double-resonance condition. The nature of this effect consists in that when the double-resonance condition is fulfilled in a narrow frequency range of the pump wave, the generation of upper-hybrid plasma oscillations is absent around the electron gyrofrequency harmonic. This significantly affects the character of interaction

between a high-power O-mode radio wave and the plasma [14]. Thus, the presence of gyroharmonic properties in the generation of artificial ionospheric irregularities is direct evidence that high-frequency plasma oscillations should be involved in this mechanism (hereafter, by the gyroharmonic properties we mean the dependence of the characteristics of artificial ionospheric irregularities on the ratio between the pump-wave frequency and the electron gyrofrequency harmonic).

When setting up the experiments, we also allowed for the fact that the effects observed during the ionospheric modification by high-power X-mode radio waves are significantly different from the effects observed when the ionosphere is affected by O-mode waves. This is due to the fact that X-mode waves do not participate in the resonant interaction with the plasma (in this case, interaction of the pump wave with the plasma) since they are reflected from the ionosphere below the plasma resonances level [18]. The action of these waves on the ionosphere is limited by the Joule heating of the plasma, the development of a self-focusing instability, and generation of artificial periodic irregularities in the field of the standing wave formed by the waves incident on and reflected from the ionosphere. From a comparison of characteristics of the ionospheric turbulence excited by a high-power radio wave for different polarizations of the pump-wave radiation we can draw certain conclusions on the role of the resonant effects during the high-power-wave — plasma interaction. On the other hand, the action by high-power X-mode radio waves which do not participate in the resonant interactions with the plasma permits one to study the phenomena stipulated only by its Joule heating and the self-focusing instability of high-power radio waves.

We note that certain conclusions on the properties of the generation mechanism of artificial ionospheric irregularities can be drawn by using the ionospheric plasma heating under conditions where the pump-wave frequency $f_{\rm h}$ is higher than the cutoff frequency f_{0F_2} of the ionospheric F_2 layer for the wave with the corresponding polarization (the so-called transmission heating). In this case, the effects related to the features of generation of artificial turbulence near the reflection height of the pump wave are absent, while the effects determined by the Joule heating of the plasma in the field of the propagating high-power radio wave are retained. When the ionosphere is affected by O-mode waves, it is also significant that the upper-hybrid resonance frequency passes through the cutoff frequency of the F_2 layer since only under the condition $f_{\rm UH} = \sqrt{f_{\rm h}^2 - f_{\rm ce}^2} > f_{0F_2}$ can we talk about a complete cessation of the resonant interaction of the O-mode waves with the ionospheric plasma.

3. RESULTS OF THE EXPERIMENTS

3.1. Modification of the ionospheric plasma under resonance conditions at the electron gyrofrequency harmonics

To determine the gyroharmonic properties of generation of artificial ionospheric irregularities in the scale range $l_\perp \approx 50$–200 m, we performed a few measurement sessions in August 2010–2013 and in September 2012. Even the first measurements showed that in the frequency range $f_{\rm h} < 4f_{\rm ce}$ the generation of irregularities becomes weaker as the frequency $f_{\rm h}$ approaches $4f_{\rm ce}$, reaches the minimum at the values of $f_{\rm h}$ slightly below $4f_{\rm ce}$, and is rapidly recovered as $f_{\rm h}$ rises in the region $f_{\rm h} \geq 4f_{\rm ce}$ [4]. The subsequent measurements permitted us to determine more accurately the properties of the observed phenomenon.

As an example, we consider the results of the studies performed in August 28, 2013. In those experiments, the ionosphere was heated by the SURA facility in the evening hours at frequencies close to the fourth harmonic of the electron gyrofrequency $4f_{\rm ce} \approx 5450$ kHz, which, according to the geomagnetic field model [19], corresponds to the altitude 210 km for the SURA facility. In those experiments, the SURA facility was operated in the 2-min emission — 2-min pause regime. During the pause, the transmitters of the facility were tuned to the next frequency; the frequency run was performed within the limits ± 100 kHz from the electron gyrofrequency harmonic. A diagram of the pump-wave frequency is shown in Fig. 1 by a solid line. The electron gyrofrequency harmonic was found according to the suppression of generation of the DM component (down-shifted maximum) in the SEE spectrum, which was recorded using an HP3885A spectrum analyzer at the SURA reception point. The behavior of the frequency $4f_{\rm ce}$ in the experiments is

shown in Fig. 1 by a dashed line. It is seen in Fig. 1 that during the experiment the pump-wave frequency passed two times through $4f_{ce}$. The frequency f_h ranged from 5365 to 5545 kHz with 20-kHz step in the first passage and with 40-kHz step in the second passage. The pump-wave frequency was close to $4f_{ce}$ in the heating cycles started at 17:54, 17:58, and 18:02 MSK in the first passage and in the heating cycles started at 18:30 MSK in the second passage.

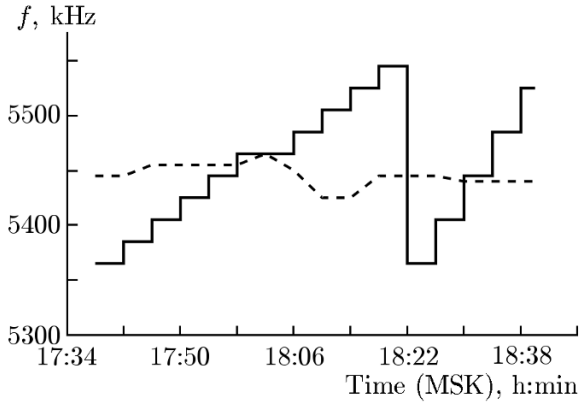

Fig. 1. Temporal dynamics of the pump-wave frequency (solid line) and the fourth harmonic of the electron gyrofrequency (dashed line) in the experiment of August 28, 2013.

The ionograms taken by the Kazan ionosonde during the experiment are presented in Fig. 2. The times at which they were obtained and the detunings $\delta f = f_h - 4f_{ce}$ are shown. Here, we consider only measurements at the time of the second passage since during measurements from 17:40 to 18:14 MSK the appearance of a strong screening sporadic E_s layer was observed, which precluded the obtaining of a full set of data. By the beginning of the second passage, the E_s layers disappeared, and ionograms which are sufficiently pure for analysis were recorded since 18:14 MSK. Figure 2*a* shows an ionogram taken at 18:19 MSK, when the pump-wave frequency was 100 kHz higher than the frequency $4f_{ce}$. Here, the scattered signal (SS) was recorded in the sounding frequency range 6–7 MHz, which corresponded to scattering by irregularities with the scales $l_\perp \approx 50$–70 m in the altitude range 255–260 km (the altitudes were determined from trajectory calculations [13] based on the density profiles retrieved from respective ionograms). When passing to the detuning $\delta f = -80$ kHz (see Figs. 2*b* and 2*c*), the weak scattered signal was seen only after the pump-wave switch-on and disappeared when the ionospheric heating was continued (the so-called overshoot effect). With the f_h increase corresponding to $\delta f = -40$ kHz, the overshoot effect disappeared, and a very weak scattered signal became seen only some time after the pump-wave switch-on (see Fig. 2*e*). For the values $\delta f = -20$ kHz, the scattered signal completely disappeared. When the frequency f_h exceeded the value $4f_{ce}$, the scattered signal in the sounding-frequency range 6–7 MHz was regularly detected over the entire range $\delta f = 5$–100 kHz, and for the detunings $\delta f = 45$ and 85 kHz the scattered signal was also received in the frequency range 3.5–5.0 MHz, where it was stipulated by irregularities with the scales $l_\perp \approx 100$ m in the altitude range 270–300 km (see Figs. 2*f*, 2*g*, and 2*h*). In all the ionograms, ovals indicate the regions where the scattered signal was recorded.

The results of all most successful experiments, in which significant results were obtained, are summarized in Table 1.

It is seen in Table 1 that for the frequencies f_h below $4f_{ce}$, the generation of artificial irregularities was absent at $\delta f = -20$ kHz and was irregular for the greater negative detuning when the scattered signal was either weak or was recorded only a short time immediately after the pump-wave switch-on (manifestation of the overshoot effect). As the frequency f_h increased in the range $f_h \geq 4f_{ce}$, the scattered-signal intensity

TABLE 1.

δf, kHz	August 26, 2013	August 27, 2013	August 28, 2013	August 26, 2010
−80		no data	weak SS	no data
−40	SS is absent	weak SS	weak SS	SS is absent
−20	SS is absent	SS is absent	no data	SS is absent
0	strong SS	strong SS	strong SS	strong SS
20	very strong SS	strong SS	no data	no data
40	very strong SS	very strong SS	strong SS	very strong SS
60	weak SS	very strong SS	no data	no data

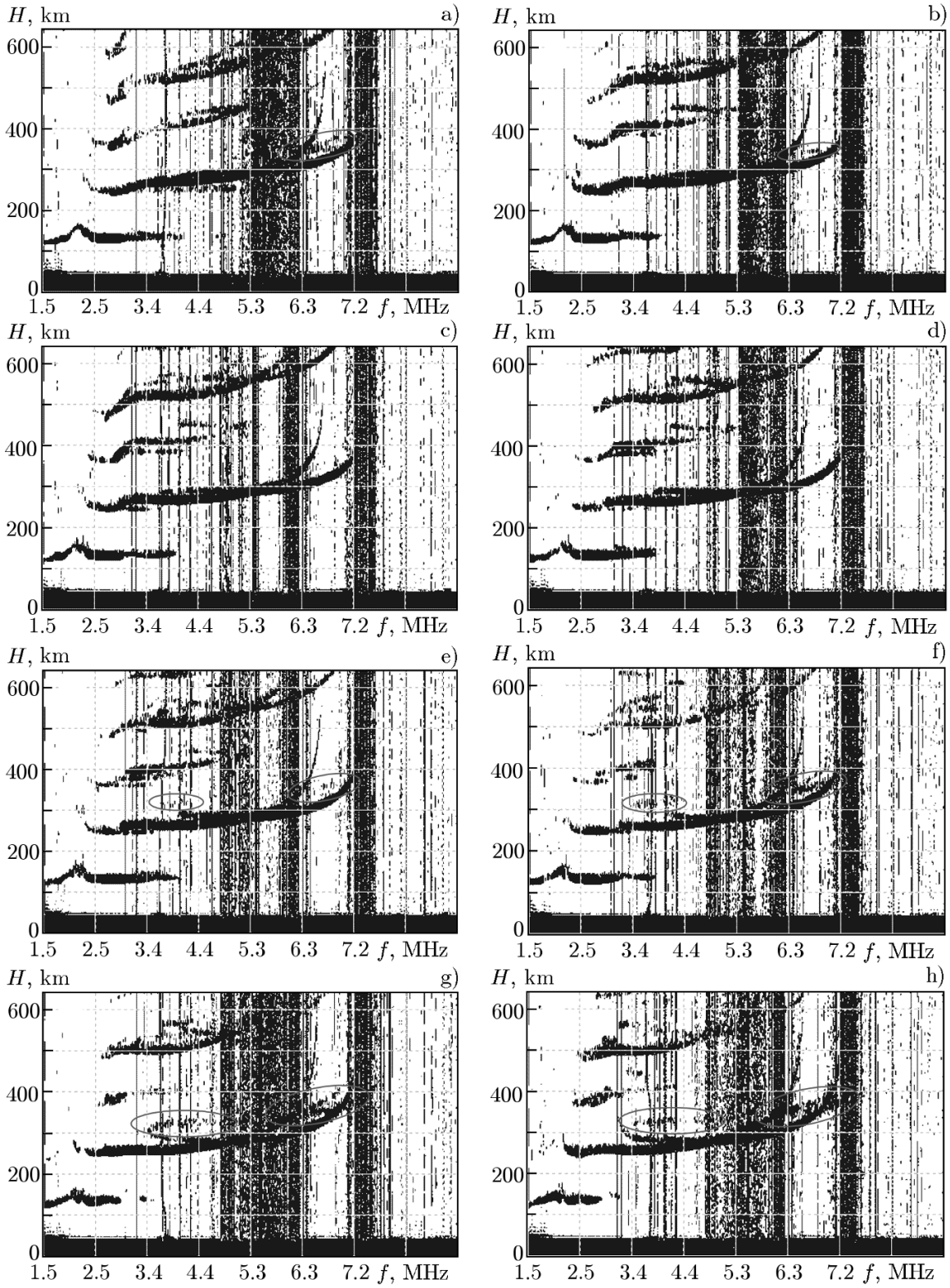

Fig. 2. A series of ionograms taken by the Kazan ionosonde during the experiment of August 28, 2013: 18:19 MSK, $\delta f = 100$ kHz (*a*), 18:22 MSK, $\delta f = -80$ kHz (*b*), 18:23 MSK, $\delta f = -80$ kHz (*c*), 18:26 MSK, $\delta f = -40$ kHz (*d*), 18:27 MSK, $\delta f = -40$ kHz (*e*), 18:32 MSK, $\delta f = 5$ kHz (*f*), 18:35 MSK, $\delta f = 45$ kHz (*g*), 18:39 MSK, and $\delta f = 85$ kHz (*h*).

rose rapidly, and at δf = 20–40 kHz it reached the values recorded far from the electron gyrofrequency harmonic. Only the measurements carried out in August 26, 2013, when the scattered signal was sharply attenuated for large positive detunings, were the exception. This was explained by the development of the sporadic E_s layer during the experiment.

Thus, the obtained experimental data demonstrate an explicit dependence of the intensity of irregularities with the scales $l_\perp \approx$ 50–100 m on the position of the pump-wave frequency with respect to the electron gyrofrequency harmonic. Such a dependence, which reflects the gyroharmonic properties in the irregularity generation, as was already mentioned, is direct evidence that the generation of irregularities with $l_\perp \approx$ 50–100 m should be related with the development of the upper-hybrid plasma turbulence, which results in the development of small-scale irregularities with $l_\perp \leq$ 50 m.

3.2. Modification of the ionospheric plasma by X-mode waves

The properties of the different-scale artificial ionospheric irregularities generated in the midlatitude ionosphere during its modification by X-mode waves was studied in [19]. It was shown in that paper that irregularities with the scales $l_\perp \approx$ 50–200 m can be excited with sufficient efficiency in the evening and nighttime conditions. Detailed study of the conditions of generation of irregularities with the scales $l_\perp \approx$ 50–100 m were performed in March, August, and September 2011 and 2012 and in September 2013. The geomagnetic disturbance level in these measurements was slightly elevated in September 26–29, 2011 and in September 2–4, 2012 (the diurnal planetary geomagnetic activity index ΣK_p in those days was within 23–32); in other days, the geomagnetic activity was very low ($\Sigma K_p \leq 10$). Over 20 measurement sessions, each having a duration of 2 to 4 h, were performed in different times of the day using different regimes of periodic radiation of a high-power radio wave from [1 min radiation — 1-min pause] to [30 min radiation,— 30-min pause]. In what follows, we consider the results of these studies, based mainly on the experiments performed in September 2011 and in March and August 2012 (when the longest measurement sessions were carried out and the most complete data sets were obtained). It should be mentioned that the generation of artificial ionospheric irregularities during the ionosphere heating by X-mode waves was mainly recorded only in the evening and nighttime hours.

Figure 3 shows a series of ionograms obtained in September 30, 2011 when the ionosphere was heated by the SURA radiation at a frequency of 5828 kHz in the [20-min radiation — 20-min pause] regime in the period from 18:50 to 19:50 MSK and the [10-min radiation — 10-min pause] regime in the period from 20:00 to 21:10 MSK. The effective radiation power was P_{eff} = 130 MW. Over the session time, the cutoff frequency f_{xF_2} for the X-mode waves decayed from 6600 to 5500 kHz, and was below the pump-wave frequency at the end of the session. In the ionograms presented here it is well seen that until the condition $f_x \leq f_{xF_2}$ is fulfilled (Figs. 3*a*–3*d*), the scattered signal is detected over the entire sounding frequency band, namely, about 50 km above the trace of the vertical sounding ionogram at effective altitudes of 290 to 330 km in the range 2–5 MHz, at altitudes of 350 to 400 km in the range 5.3–6.4 MHz as an additional trace departing from the O-trace of the ionograms, and at altitudes of 360 to 500 km in the range 6–7 MHz as an additional trace departing from its X trace. These regions of the scattered signal detection are marked in Fig. 3*b* by three ovals. The intensity of scattered signals when passing to $f_x > f_{0F_2}$ almost did not change. From this it can be concluded that indeed these irregularities are excited by X-mode waves, rather than by the residual (up to 10–15%) O-mode radiation accompanying the X-mode radiation because of the non-ideal polarization isolation of the radiating array of the heater. Scattering intensity in the frequency range 5.3–7.0 MHz rises gradually as the frequency f_x approaches the frequency f_{xF_2} (Figs. 3*b* and 3*c*), but disappears at frequencies of 2 to 5 MHz, for which the scattering occurs at altitudes between the E and F_2 layers by irregularities with the scales $l_\perp \approx$ 100–200 m. This is due possibly to both a variation in the refraction conditions leading to the violation of the scattering aspect ratio conditions and an increase in the distance from the pump-wave reflection altitude to the generation region of these irregularities, which can lead to a decrease in their generation efficiency at these altitudes. Scattering is no longer detected (the scattering intensity from the

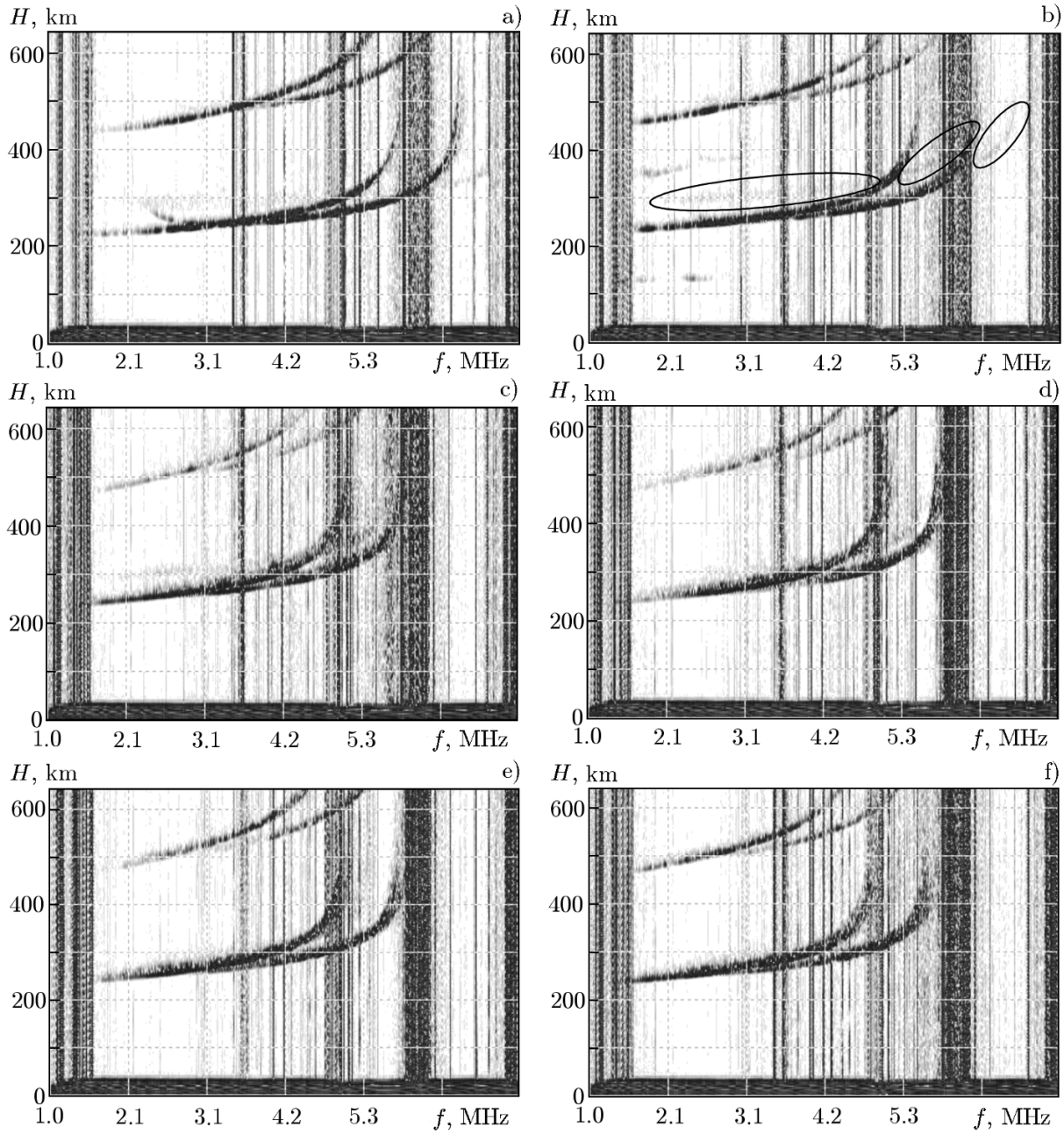

Fig. 3. A series of ionograms taken by the Kazan ionosonde during the experiment on ionospheric heating by X-mode waves on September 30, 2011: at 18:56 MSK (*a*), 19:41 MSK (*b*), 20:46 MSK (*c*), 20:51 MSK (*d*), 20:56 MSK (*e*), and 21:01 MSK (*f*).

altitudes of the ionospheric F_2 region abruptly decreases) when passing to $f_{\mathrm{x}} > f_{\mathrm{x}F_2}$, i. e. the transmission heating (Figs. 3*e* and 3*f*).

Thus, the obtained results clearly indicate that irregularities with the sizes $l_\perp \approx 50$–200 m are also generated during ionospheric modification by high-power X-mode radio waves, when the effects of resonant interaction with the plasma are absent. It should also be emphasized that for their generation it is important that the condition of reflection of a high-power X-mode radio wave from the ionospheric F_2 region should be fulfilled.

Comparison of the irregularity intensities calculated from ionograms and measured in similar conditions using high-power O- and X-mode radio waves for the ionospheric modification shows that during

heating by X-mode waves the intensity of irregularities is only a factor of 3 to 5 smaller than during heating by O-mode waves, which coincides with the measurement results obtained previously [20]. This indicates that when the ionosphere is affected by O-mode waves, the generation of artificial irregularities is determined by several mechanisms.

We note once again that in the results presented in this section the generation of artificial irregularities with $l_\perp \approx 50$–200 m in the absence of resonant interaction of radio waves with the ionospheric plasma (during ionospheric modification by high-power X-mode radio waves) was observed only in the evening and nighttime conditions. This explains the absence of such an effect in the O-mode measurements described in Sec. 3.1 where the experiments were carried out in a still illuminated ionosphere.

3.3. Modification of the ionospheric plasma by O-mode waves

Consider the features of the wave scattering and, therefore, generation of artificial irregularities with $l_\perp \approx 50$–200 m in the ionosphere modified by high-power O-mode radio waves under conditions where the pump-wave frequency first becomes equal to and then greater than f_{0F_2} as the cutoff frequency f_{0F_2} is decreased. When passing through the cutoff frequency, there is no abrupt decrease in the intensity of the scattered signal; the latter continues to be detected until the pump-wave frequency exceeds the value of f_{0F_2} at 100–200 kHz, i. e. until the upper-hybrid resonance frequency remains less than the cutoff frequency f_{0F_2}. Such a character of generation of the upper-hybrid turbulence was mentioned many times before (see, e. g., [17, 21]).

The studies of the ionospheric modification by high-power O-mode radio waves in March 2014 have shown that the relaxation time of irregularities with the scales $l_\perp \approx 50$–200 m strongly increases when passing from the evening to nighttime conditions of measurement. The relaxation time is about 1 min on the time interval from 20:00 to 23:00 MSK, increases up to 2 min at 24:00 MSK, and can amount to tens of minutes in the midnight hours when the development of natural F spread is observed in the vertical sounding ionograms. These results directly indicate that the dynamics of the studied irregularities can be affected by kilometer-scale irregularities of both natural and artificial origin. The results of studying the dynamics of these irregularities in the transition from day to night on the same scattering path are presented in [22]. On the whole, the conclusions drawn in [22] and the conclusions that follow from our measurements agree with each other. In [22], the slowing down of the relaxation of irregularities in the late evening and nighttime hours is attributed to an increase in their longitudinal sizes in the transition from day to night.

4. CONCLUSIONS

The results of our studies suggest that the generation of artificial ionospheric irregularities with the scales $l_\perp \approx 50$–200 m at the altitudes of the ionospheric F_2 region occurs when the ionosphere is modified by both O- and X-mode high-power radio waves. In the first case, the gyroharmonic properties of the irregularities are evidence that their generation should be related with the development of the upper-hybrid plasma turbulence and excitation of small-scale ($l_\perp \leq 50$ m) irregularities. In the case of X-mode waves, the resonant interaction between a high-power radio wave and the plasma is not possible and the generation of these irregularities should be determined by the Joule heating of the plasma and self-focusing instability of the beam of high-power radio waves.

Thus, it can be assumed proved that there exist at least two mechanisms for generation of artificial ionospheric irregularities with the scales $l_\perp \approx 50$–200 m in the ionospheric F_2 region near the reflection level of a high-power radio wave. Recall that these scales in the spectrum of artificial ionospheric irregularities lie between the spectral maximum in the region $l_\perp \approx 50$ m, which is related to the development of small-scale irregularities as a result of the development of a thermal (resonant) parametric instability, and the maximum in the region $l_\perp \approx 500$ m, which is due to the self-focusing instability of the beam of high-power radio waves. In the first case, the development of a parametric instability is possible only when the ionosphere is modified by O-mode high-power radio waves. In the second case, the formation of irregularities takes place when

waves of both polarizations are used, but the plasma stratification is more intense in the case of O-mode waves because of the stronger heating of the plasma by a high-power radio wave and the magnetic zenith effect [23]. We emphasize that in both cases, the presence of the pump-wave reflection in the Earth's ionosphere has a significant effect on the development of these instabilities. It can be supposed that the generation of irregularities with the scales $l_\perp \approx$ 50–200 m is due to the nonlinear cascade [24] over the turbulence spectrum both from the side of the spectral maximum in the region $l_\perp \approx 50$ m and from the side of the maximum in the region $l_\perp \approx 500$ m. At least, this does not contradict all the available experimental data on the irregularity properties considered in this paper.

The mechanism of generation of irregularities with the scales $l_\perp \approx$ 100–200 m at altitudes of 100 to 150 km should be considered separately. It was shown in [25–28] that these irregularities cannot appear due to their extension from the reflection height of a high-power radio wave, where the most intense artificial ionospheric irregularity is generated and artificial ionospheric irregularities with different scales develop. Judging by the results of [28], these irregularities appear at such low altitudes almost immediately with the development of irregularities at the altitudes of the ionospheric F_2 region. Their formation is due most probably to the generation of irregularities in the ionospheric E layer, the mechanism of which has not been fully examined to date. The corresponding experimental and theoretical studies are still ahead.

The authors are grateful to the SURA facility collaborators for help with the experimental studies.

The work by V. L. Frolov, A. D. Akchurin, and E. Yu. Zykov was done at the expense of a subsidy allocated within the framework of State support of the Kazan (Volga) Federal University in order to improve its competitiveness among the world's leading research and education centers. The work by I. A. Bolotin was supported by the Russian Science Foundation (project No. 14–12–00556) with regard to processing and analysis of the experimental data. Most of the experiments under the research program were conducted in 2010–2013 with financial support of the "Geofizika" Federal Target Program and the Russian Foundation for Basic Research (project Nos. 11–02–00374, 12–02–31839, 12–05–33065, 13–05–01122, 13–05–00511, 13–02–12074, and 13–02–12241).

REFERENCES

1. L. M. Erukhimiov, S. A. Metelev, E. N. Myasnikov, et al., *Radiophys. Quantum Electron.*, **30**, No. 2, 156 (1987).
2. V. L. Frolov, L. M. Erukhimov, S. A. Metelev, amd E. N. Sergeev, *J. Atmos. Solar-Terr. Phys.*, **59**, No. 18, 2317 (1997).
3. E. M. Allen, G. D. Thome, and P. B. Rao, *Radio Sci.*, **9**, No. 11, 905 (1974).
4. J. Minkoff, *Radio Sci.*, **9**, No. 11, 997 (1974).
5. S. M. Grach, A. N. Karashtin, N. A. Mityakov, et al., *Sov. J. Plasma Phys.*, **4**, 737; 742 (1978).
6. V. V. Vas'kov and A. V. Gurevich, *Sov. Phys. JETP*, **42**, 91 (1975).
7. A. C. Das and J. A. Fejer, *J. Geophys. Res.*, **A84**, 6701 (1979).
8. A. G. Litvak, *Radiophys. Quantum Electron.*, **11**, No. 9, 814 (1968).
9. F. W. Perkins and E. J. Valeo, *Phys. Rev. Lett.*, **32**, 1234 (1974).
10. V. V. Vas'kov and A. V. Gurevich, *Radiophys. Quantum Electron.*, **18**, No. 9, 929 (1975).
11. L. M. Erukhimov, G. P. Komrakov, and V. L. Frolov, *Geomagn Aéron.*, **20**, No. 6, 1112 (1980).
12. N. A. Zabotin, A. G. Bronin, G. A. Zhbankov, et al., *Radio Sci.*, **37**, No. 6, 1102 (2002).
13. I. A. Bolotin, V. L. Frolov, A. D. Akchurin, et al., *Radiophys. Quantum Electron.*, **55**, Nos. 1–2, 59 (2912).
14. S. M. Grach, B. Thidé, and T. B. Leyser, *Radiophys. Quantum Electron.*, **37**, No. 5, 392 (1994).

15. V. L. Frolov, E. N. Sergeev, E. N. Ermakova, et al., *Geophys. Res. Lett.*, **28**, No. 16, 3103 (2001).
16. E. N. Sergeev, V. L. Frolov, S. M. Grach, and P. V. Kotov, *Adv. Space Res.*, **38**, 2518 (2006).
17. T. B. Leyser, *Space Sci. Rev.*, **98**, 223 (2001).
18. V. L. Ginzburg, *The Propagation od Electromagnetic Waves in Plasmas*, Pergamon Press, Oxford (1970).
19. http://ccmc.gsfc.nasa.gov/modelweb/models/igrf_vitmo.php
20. V. L. Frolov, I. A. Bolotin, G. P. Komrakov, et al., *Radiophys. Quantum Electron.*, **57**, No. 6, 393 (2014).
21. N. F. Blagoveshchenskaya, H. C. Carlson, V. A. Kornienko, et al., *Ann. Geophys.*, **27**, 131 (2009).
22. E. N. Sergeev, E. Yu. Zykov, A. D. Akchurin, et al., *Radiophys. Quantum Electron.*, **55**, Nos. 1–2, 71 (2012).
23. A. V. Gurevich, *Phys. Usp.*, **50**, No. 11, 1091 (2007).
24. N. D. Filipp, N. Sh. Blaunshtein, L. M. Erukhimov, et al., *Modern Methods for Studying Dynamic Processes in the Ionosphere* [in Russian], Shtiinitsa, Kishinev (1991).
25. N. V. Bakhmet'eva, N. P. Goncharov, Yu. A. Ignat'ev, G. S. Korotina, et al., *Geomagn. Aéron.*, **29**, No. 5, 799 (1989).
26. N. V. Bakhmet'eva, S. A. Dmitriev, Yu. A. Ignat'ev, and P. B. Shavin, *Geomagn. Aéron.*, **32**, No. 3, 180 (1992).
27. N. V. Bakhmet'eva, V. D. Vyakhirev, et al., *Radiophys. Quantum Electron.*, **53**, Nos. 5–6, 305 (2010).
28. N. V. Bakhmet'eva, V. L. Frolov, V. D. Vyakhirev, et al., *Radiophys. Quantum Electron.*, **55**, Nos. 1–2, 95 (2012).